

¹ Department of Atmospheric Environmental Sciences, Kangnung National University, Kangnung, Korea

² State Key Joint Laboratory of Environmental Simulation and Pollution Control, College of Environmental Sciences, Peking University, Beijing 100871, People's Republic of China

³ Centre for Environmental Modelling and Prediction, School of Mathematics, The University of New South Wales, Sydney, Australia

Effects of atmospheric circulation and boundary layer structure on the dispersion of suspended particulates in the Seoul metropolitan area

H. Choi^{1,2} and M. S. Speer³

With 19 Figures

Received October 24, 2004; accepted April 12, 2005

Published online: October 27, 2005 © Springer-Verlag 2005

Summary

A three-dimensional non-hydrostatic numerical model and lagrangian particle model (random walk model) were used to investigate the effects of the atmospheric circulation and boundary layer structure on the dispersion of suspended particulates in the Seoul metropolitan area. Initially, emitted particulate matter rises from the surface of the city towards the top of the convective boundary layer (CBL), owing to daytime thermal heating of the surface and the combined effect of an onshore wind with a westerly synoptic-scale wind. A reinforcing sea-valley breeze directed from the coast toward the city of Seoul, which is enclosed in a basin and bordered by mountains to its east, disperses the suspended particulate matter toward the eastern mountains. Total suspended particulate concentration (TSP) at ground level in the city is very low and relatively high in the mountains. Radiative cooling of the surface produces a shallow nocturnal surface inversion layer (NSIL) and the suspended particulate matter still present near the top of the CBL from the previous day, sinks to the surface. An easterly downslope mountain wind is directed into the metropolitan area, transporting particulate matter towards the city, thereby recycling the pollutants. The particulates descending from the top of the NSIL and mountains, combine with particulates emitted near the surface over the city at night, and under the shallow NSIL spread out, resulting in a maximum ground level concentration of TSP in the metropolitan area at 2300 LST. As those particles move toward the Yellow Sea through the topographically

shaped outlet west of Seoul city under the influence of the easterly land breeze, the maximum TSP concentration occurs at the coastal site. During the following morning, onshore winds resulting from a combined synoptic-scale westerly wind and westerly sea breeze, force particulates dispersed the previous night to move over the adjacent sea and back over the inland metropolitan area. The recycled particulates combine with the particulates emitted from the surface in the central part of the metropolitan area, producing a high TSP and again rise towards the top of the CBL ready to repeat the cycle.

1. Introduction

As there is a population of twelve million people and two and a half million vehicles in the Seoul metropolitan area, a large amount of pollution including particulates are emitted at the surface. Owing to the Seoul city basin being surrounded by mountains and open to the sea at its western outlet, the diurnal variation of pollutant concentration is very complicated. The concentrations of emitted particulates or gases are greatly affected both by diurnal variations in atmospheric circulation and the depth of the atmospheric boundary layer.

Lyons and Olsson (1973) indicated the effects of meteorological conditions on air pollution dispersion in the Chicago lakes and basin area using a three-dimensional meteorological model. Ross et al (1999) explained that the local airshed surrounding the Comalco smelter was strongly influenced by the proximity of the ocean and the complex terrain of the Tama Valley, producing complex interactions with the sea breeze, cold drainage winds and the channelling of winds by topography.

Local circulation systems are complicated in the presence of complex terrain and adjacent sea under differing weather conditions (Choi, 2001; Kimura, 1983; Kuwagata and Sumioka, 1991). Baird (1995) explained the increase in pollution concentration under daytime photochemical reaction processes in a city environment. Moller (2001) concluded that pollutant gases could be changed into the aerosol phase through their chemical reaction processes and cause an increase in local and regional air pollution concentrations that result in an interruption of the local radiation balance. Park and Moon (2001) calculated particle dispersion in the complex coastal terrain of Korea using a lagrangian particle model.

Suspended particulates are not only harmful to human health but also of great importance in some natural atmospheric processes involving the heat budget in the atmospheric boundary layer. A high density of suspended particulates near the top of the convective boundary layer (CBL) reduces the solar energy reaching the ground and the reduction of solar radiation interrupts daytime convective processes near the surface, resulting in a decrease in vertical mixing depth of air in the boundary layer and an increase in TSP (Xuan, 1999).

Computation of the dust emission factors of Seoul is very difficult owing to the lack of necessary input data such as emission rate, chemical processes among different species, meteorological impact on the transportation and diffusion of particulates. Another example of high TSP is that of particulates in the air reducing rainfall acidity in Northern China, due to the presence of alkaline components (PU, 1995). However, that study was mainly confined, not to particulates emitted in the city, but sandstorm particulates transported from the Gobi desert in Mongolia.

The purpose of this study is to investigate how wind, atmospheric boundary layer structure, topography and sea can have important roles for the occurrence of high nocturnal concentrations of TSP, especially focusing on dry depositional processes, using both a three dimensional meteorological model and a random walk (or lagrangian particle) model.

2. Data collection and numerical method

2.1 Topographical features of sampling site

Topographical features of the Seoul metropolitan area (centred on 37°34' N, 126°58' E) consist of the Yellow Sea in the west, the Seoul basin in the centre and high mountains surrounding the city in the east (Fig. 1). The Seoul city basin extends to just less than 200 m in height, and is shaped like the top of a jug with a drainage outlet on the western side leading to the Yellow Sea. Further inland lies Mt. Yongmoon (height 1,150 m), as indicated in the fine-mesh domain (Fig. 3). Thus, the climate near Seoul city is generally affected by both sea and mountains that can produce temperature contrasts resulting in diurnal wind regimes. Owing to the complex topographical features of the mountains surrounding Seoul city to the north, east and south, and its western outlet stretching over the coastal plain to the sea, the diurnal variation of pollutant concentration is very complicated. This variation is due to two factors: (1) wind direction and, (2) the depth of the atmospheric boundary layer.

2.2 Numerical model and input data

A three-dimensional non-hydrostatic grid point model in a terrain following coordinate system (x, y, z^*) called LAS-V, which was originally developed by the Meteorological Research Institute (MRI), Japan Meteorological Agency (JMA) was adapted to investigate not only the large scale atmospheric circulation in north eastern Asia and local scale circulations in the mountainous coastal regions, but also to investigate the structure of the atmospheric boundary layer. The numerical simulation was performed using a Hitachi super computer at MRI. Two different domains each consisting of 50×50 grid points were used with a uniform horizontal interval of

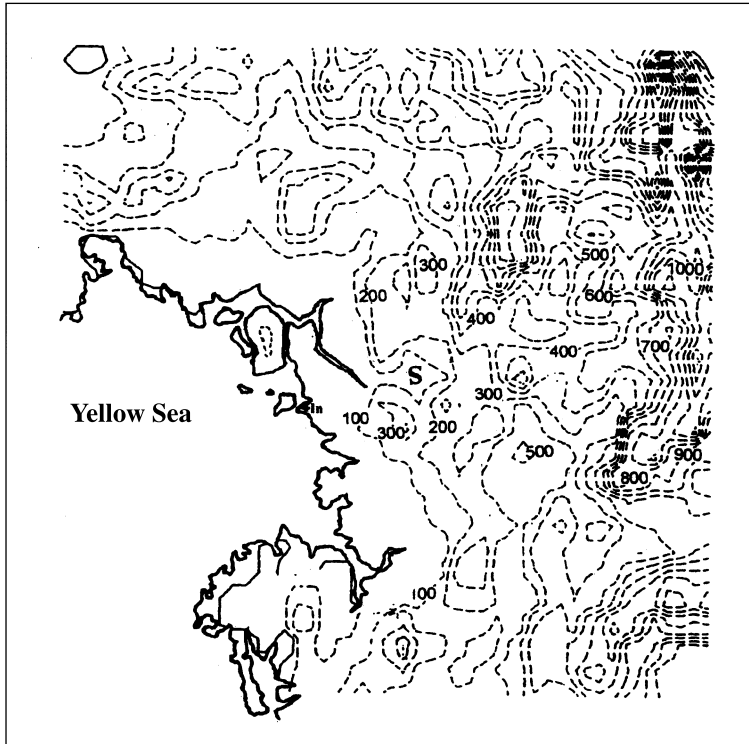


Fig. 1. Map of topography (m) surrounding Seoul city in the fine-mesh domain (5 km) of the numerical model. S denotes the Seoul metropolitan area. Contour interval = 100 m

20 km (coarse-mesh) and 5 km (fine-mesh), respectively, and one-way double nesting. For the two domains, 16 vertical levels were spaced from a height of 10 m above ground to 6 km (the top of our model domain) with sequentially larger intervals in the upper layers.

Every twelve hourly global JMA analysis (G-ANAL), at a horizontal resolution of 1.25° , consisting of atmospheric pressure, wind, potential temperature and specific humidity on five vertical levels from the surface to 100 hPa level (approximately 13 km), was horizontally and vertically interpolated onto the sixteen levels of the two models. The predicted fields from the coarse-mesh domain were treated as lateral boundary conditions for the fine-mesh domain. Sea surface temperature values that were derived from GMS and NOAA satellite images and re-analyzed by the National Fisheries Research and Development Agency of Korea (NFRDA, 1998), were used as initial input data in the two model domains.

The LAS-V model consists of three-dimensional hydrostatic and non-hydrostatic options with a terrain following coordinate system (x, y, z^*) based upon the Boussinesq and anelastic approximations (Kimura and Arakawa, 1983; Kimura and Takahashi, 1991; Takahashi, 1998). The equation

of motion contains $u, v, w, w^*, \theta, \Theta, T, \pi, \pi_m, \pi', z, z_T, z_G, K_m$ and K_h , which denote x -, y -, z - and z^* -components of wind velocity, potential temperature ($\theta = T(1000 P^{-1})^{Rd/Cp}$, $\theta' = \theta - \Theta$), mean potential temperature of the model domain, air temperature at a given height, Exner function of hydrostatic pressure in the model atmosphere ($\pi = C_p (P/P_{00})^{Rd/Cp}$), Exner function of hydrostatic pressure in the isentropic atmosphere ($\theta = \Theta$), deviation of π , height of upper boundary with its change in time and space in the model domain, height of topography and vertical diffusion coefficient for turbulent momentum and heat ($m^2 s^{-1}$), respectively. The height on the terrain-following vertical coordinate is defined as $z^* = z_T (z - z_G) h^{-1}$, where $h = z_T - z_G$.

Pressure equations can be converted by the hydrostatic pressure deviation, π' ($=\pi - \pi_m$) and non-hydrostatic pressure obtained from the hydrostatic pressure (π'_H) in the non-hydrostatic calculation, (π'_N) ($=\pi' - \pi'_H$). Radiative heating of air and specific humidity of water vapor are evaluated from the thermodynamic equation and the conservation of water vapor, q . For the time integration and the vertical z^* -coordinate, the Euler-backward scheme and the Crank-Nicholson scheme are adopted, respectively. Relaxation of the radiative condition according to Klemp and Durran (1983)

was applied to the atmospheric pressure changes at the top of the model. Also, the periodic lateral boundary condition of Orlandi (1976) was applied to the calculation of u , v , θ and q . In the surface boundary layer, vertical diffusion coefficients, K_m and K_h for momentum and heat are evaluated from the turbulent closure level-2 model (Yamada, 1983; Yamada and Mellor, 1983).

The simplified scheme of Katayama (1972) that computes radiative transfer in the troposphere is used to evaluate total net flux of long wave radiation absorbed by both H_2O and CO_2 and the flux from the surface toward the upper levels is taken to have a positive sign with regard to H_2O - and CO_2 -transmission functions, effective vapour amount, specific humidity and pressure. Similarity theory is adopted for the energy budget near the surface, and the surface boundary layer is assumed to be a constant flux layer in order to estimate sensible and latent heat fluxes (Businger, 1973; Monin, 1970). The force restore method of Deardorff (1978) was employed on the diurnal variation of soil temperature and specific humidity at the surface. The solutions of equations for the time integration and the vertical direction (z^* -coordinate) were calculated by the Euler-backward scheme and Crank-Nicholson scheme. The calculation time interval was given as $\Delta t = 30$ s in the coarse-mesh domain and $\Delta t = 10$ s in the fine-mesh domain.

A random walk model (or lagrangian particle model) developed by the Meteorological Research Institute of Japan has a terrain following coordinate system (x , y , z^+) and was used to investigate the dispersion and diffusion of suspended particulate matter originating from the surface. Meteorological elements such as wind and vertical diffusion of turbulent momentum evaluated by the meteorological model were supplied to the random walk model as input data. The random walk model was then used for tracing the lagrangian motion of particle diffusion by transforming three-dimensional wind and turbulence fields calculated from the z^* -coordinate system (x , y , z^*) into z^+ (x , y , z^+) for the conservation of pollutant masses in the particle dispersion model.

Emission data could not be used owing to the uncertainty associated with estimating the data by simple statistical methods. This included calculating the amount of TSP emissions by estimating

the number of vehicles and factories and other sources. Thus, four particles were released every two minutes in the daytime and two particles at night, in order to investigate the transportation and diffusion patterns of suspended particulates under the influence of the atmospheric circulation and boundary layer structure due to topography and the heat budget in the study area.

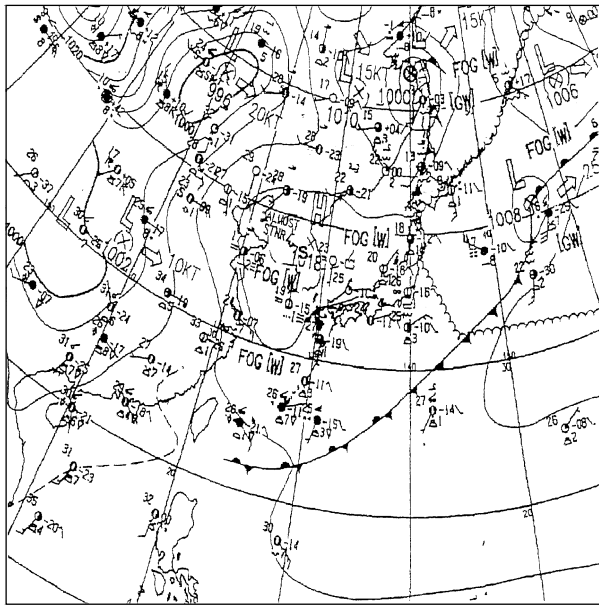
Hourly data of total suspended particulate concentration from 0100 LST on 20 May to 0900 LST, 22 May, 1998 were automatically measured by high-volume and low-volume air samplers (DASBI-1108). This measuring apparatus was located at Kagwamoon, a monitoring site operated by the Seoul Regional Environmental Administration, Ministry of Environment of the Korean Government in Seoul City (MOE, 1998). The number of particles calculated from numerical modelling results could not be directly compared with observed concentrations of TSP matter measured at the observation point. However, the temporal trends of the density of particles at ground level across the metropolitan area could be compared with those of the TSP concentrations. This is because the main purpose of this study is to investigate to what extent the atmospheric circulation and boundary-layer structure can affect the dispersion of suspended particulates in the city, subject to the effects of the surrounding mountains and western outlet that leads to the sea.

3. Results

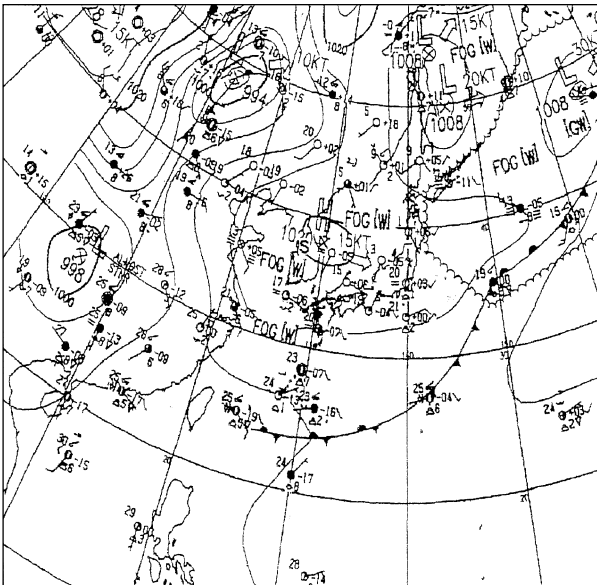
3.1 Daytime atmospheric circulation and boundary layer

Every 12 hours the coarse-mesh domain forecasts were used as boundary conditions for the fine-mesh domain covering the 48 hours from 0900 LST, May 19 to 0900 LST, May 21, 1998. In order to verify the atmospheric circulation and heat budget near the Seoul metropolitan area and to describe their forcing mechanisms for a period of a single day, the simulation results from 1200 LST, 20 May 20 to 0600 LST, 21 May are illustrated here.

The SLP chart at 1500 LST, 20 May, 1998 (Fig. 2a), shows that the centre of a high-pressure was located in the central eastern part of the Korean peninsula, and a synoptic-scale south to



a

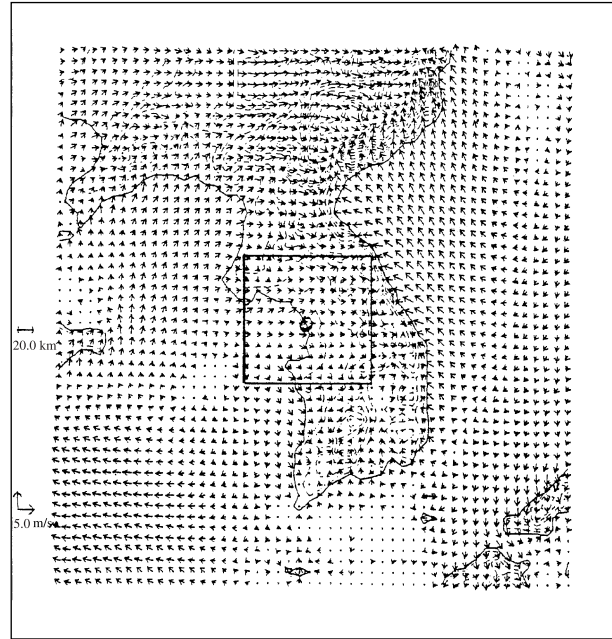


b

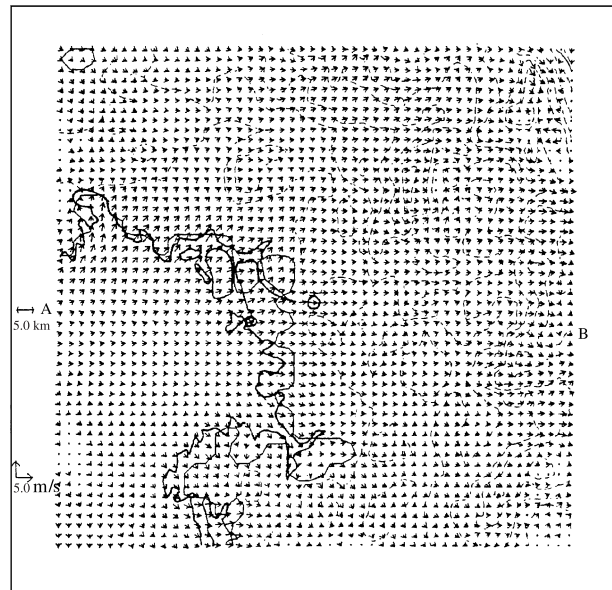
Fig. 2a. SLP chart showing selected observations at 1500 LST, 20 May, 1998, **(b)** as in **(a)** except at 2100 LST, 20 May. “S” in the central part of the map denotes Seoul city

south-westerly wind prevailed near Incheon city in the central part of the western coast of Korea. At 2100 LST, although the high-pressure centre had moved toward the eastern coast of Korea, synoptic scale south-westerly winds still prevailed near Incheon city (Fig. 2b). As a first step, wind fields were analyzed to investigate the relationship of winds on the synoptic, meso- and micro-scales. In the coarse-mesh domain, divergence of wind

fields driven by a high-pressure occurs around the central part of the Yellow Sea and the wind speed increases away from the high-pressure centre (Fig. 3a). Synoptic-scale westerly winds combined with downward motion and a meso-scale



a

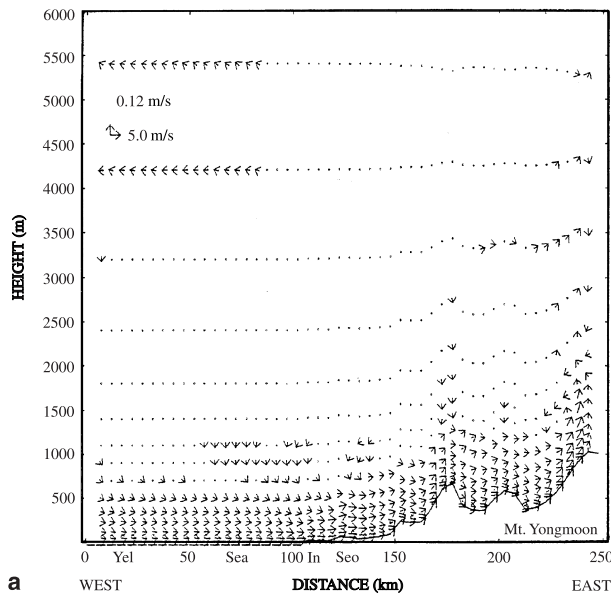


b

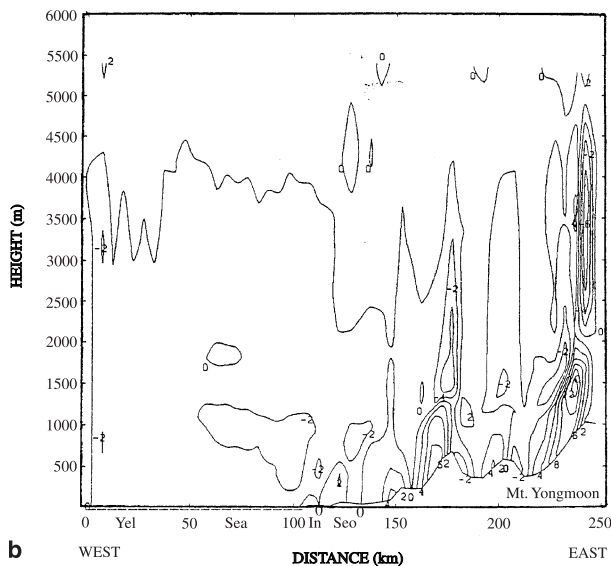
Fig. 3a. Wind vectors (m s^{-1}) at 10 m above ground level in the coarse-mesh domain (20 km) near the Korean peninsula at 1200 LST, 20 May, 1998, **(b)** as in **(a)** except in the fine-mesh domain (5 km). The inset in **(a)** denotes the fine mesh domain in **(b)**. Dashed lines denote topographical contours. Two small circles in **(b)** denote Incheon city (left) and Seoul city (right)

westerly sea-breeze in daylight hours, resulted in a moderate onshore wind on the western coast of Korea (Fig. 3b).

Figure 4a shows the vertical wind profile (m s^{-1}) on the line A–B in Fig. 3b. The onshore wind combined with the synoptic scale westerly and enhanced further by the sea-breeze, resulted in an intensified westerly wind regime directed from the inland basin toward the top of the mountains. The onshore wind was moderate near



a

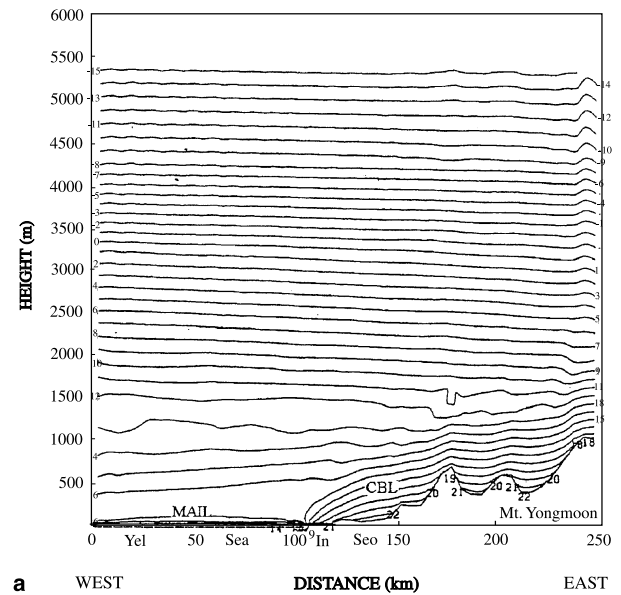


b

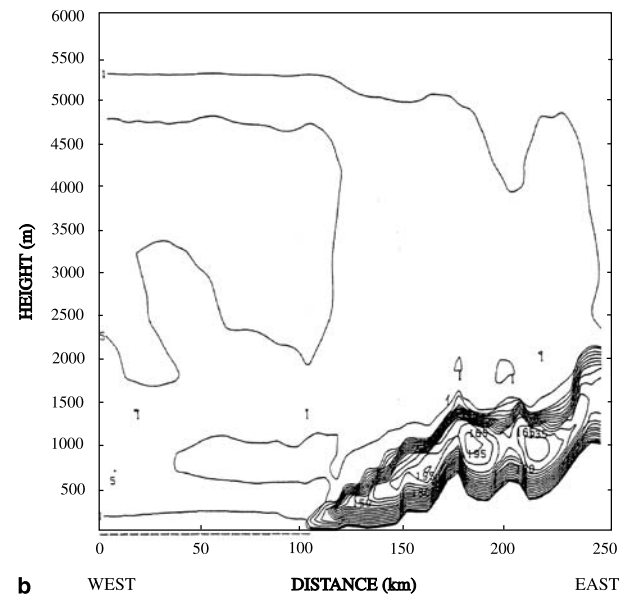
Fig. 4a. Vertical wind profile (m s^{-1} , horizontal scale and cm s^{-1} , vertical scale) on a line A–B in Fig. 3b. Yel, Sea, In and Seo denote the Yellow Sea, coastal sea, Incheon and Seoul cities, respectively. **(b)** Contours of vertical wind speed (cm s^{-1}), negative value denoting downward motion. Dashed line from 0 to 100 on the bottom axis indicates sea

Inchon (In), but relatively strong near Seoul (Seo) under the influence of the valley wind. Thus, a localized westerly wind prevailed in the Seoul metropolitan area, which is surrounded by mountains. Figure 4b shows a vertical profile of wind speed (cm s^{-1}), negative values indicating downward motion.

Under the development of a thermal internal boundary layer (TIBL) from the coastal fringe toward the inland basin, and convective boundary



a

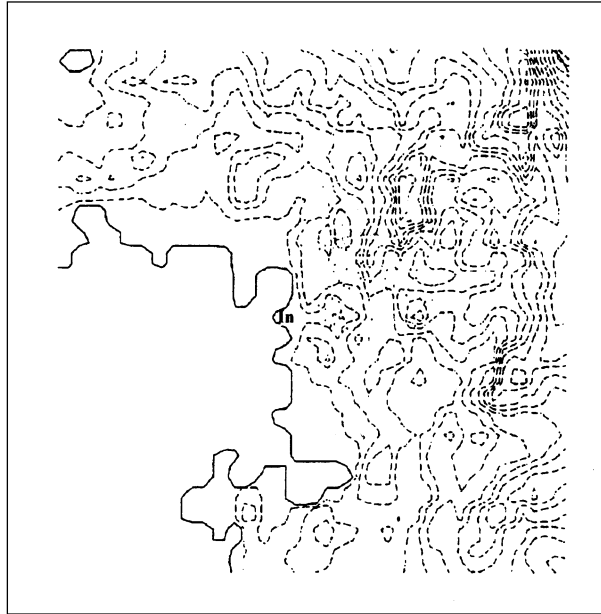


b

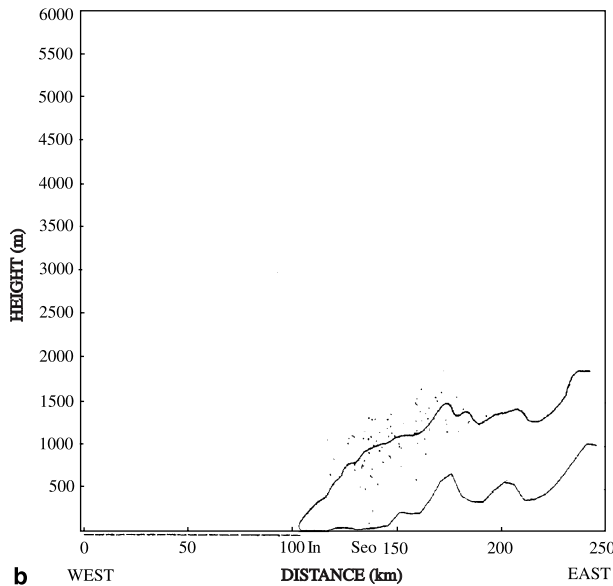
Fig. 5a. As shown in Fig. 4a except for air temperature ($^{\circ}\text{C}$) and **(b)** vertical diffusion coefficient of turbulent heat ($\text{m}^2 \text{s}^{-1}$). CBL and MAIL denote convective boundary layer and marine atmospheric inversion layer, respectively

layer (CBL) to a depth of approximately 800 m from the inland part of the basin toward the mountains, most of the water vapour near the surface was evaporated to the top of the boundary layer, a height at which the air temperature becomes uniformly constant (Fig. 5a). Much more water vapour needs to be supplied for the con-

densation of surface water vapor at the coastal edge of the basin. The vertical distribution of turbulent diffusion coefficient for heat, K_h , showed that the CBL due to thermal convection was strongly developed from the coast toward the inland (Fig. 5b), resulting in high air temperatures at the coast and further inland.

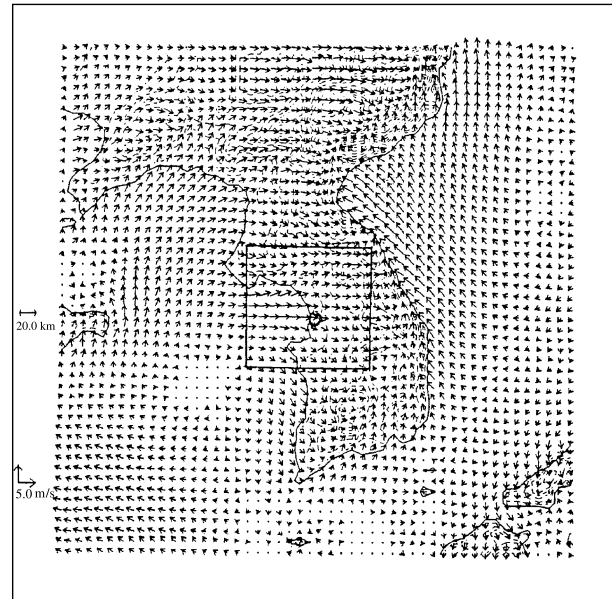


a

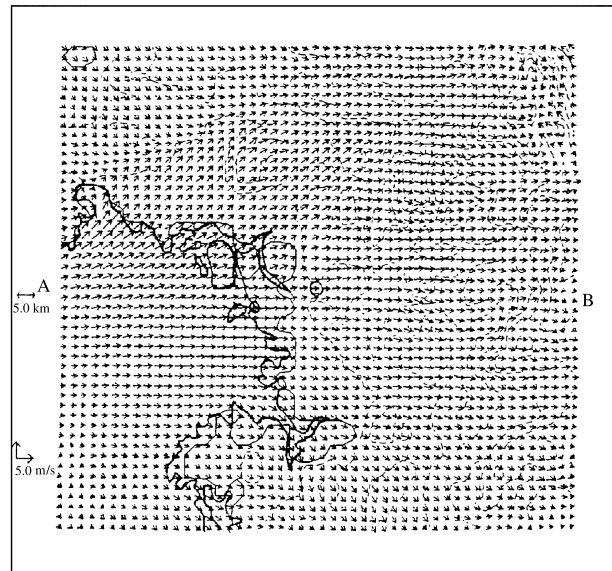


b

Fig. 6a. Plan view showing transport of particulates near Seoul city at 1200 LST, on 20 May, 1998, six hours after releasing particulates. “In” denotes Incheon city and the diamond shaped topographical contour area to the right of Incheon city indicates Seoul city. **(b)** as in **(a)**, except vertical cross-section through Incheon city and Seoul city. Upper and lower lines indicate the top of the CBL and topography, respectively



a



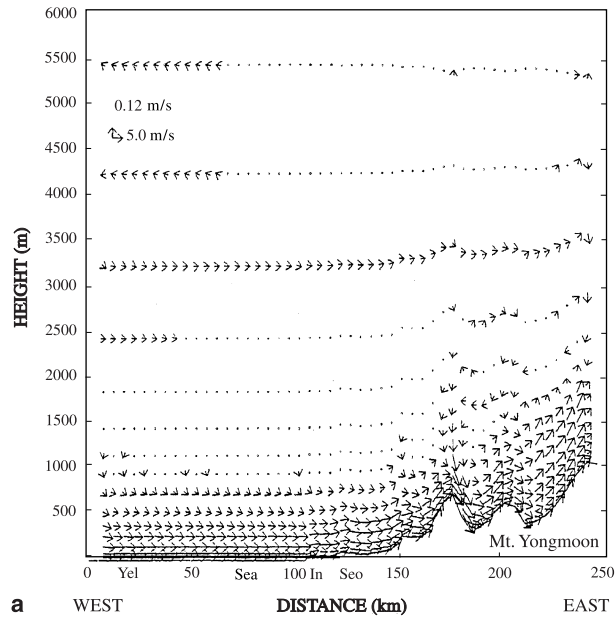
b

Fig. 7. Wind vectors (m s^{-1}) 10 m above ground level at 1800 LST, 20 May, 1998 in, **(a)** the coarse-mesh domain (20 km) near the Korean peninsula. The inset and dashed lines denote the fine-mesh domain and topographical contours, respectively. The open circle denotes Incheon city. **(b)** as in **(a)**, except the fine mesh domain indicated by the inset in **(a)**. The open circle denotes Seoul city

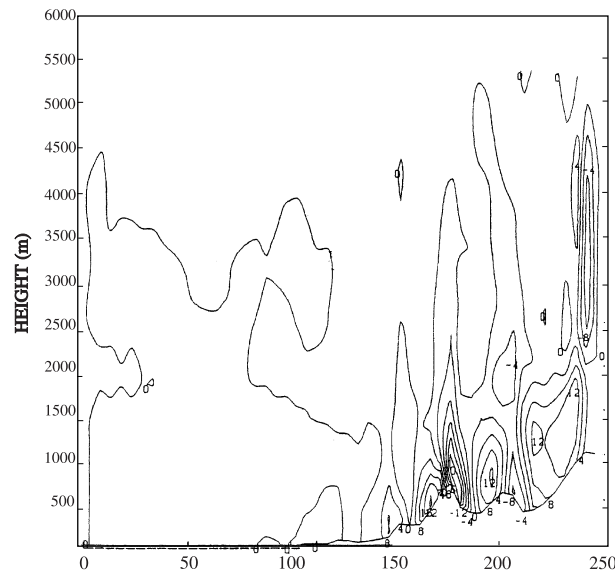
3.2 Daytime dispersion of suspended particulate

In order to investigate the dispersion and diffusion of particulates due to atmospheric boundary layer forcing, particles were initially released at a rate of four per two minutes from 0600 LST in the central part of Seoul city. The releasing con-

tinues until the numerical simulation finishes. Initially, emitted particulate matter remained suspended due to thermal convection in the metropolitan area from the surface to the top of the CBL and under westerly winds it was dispersed eastward below the height of the sea-breeze front and within the CBL. The particles were then transported upslope and widely dispersed over the mountains surrounding Seoul city. TSP concentration near the surface of the Seoul metropolitan area at 1200 LST was very low and relatively high over the mountains (Fig. 6a and b).

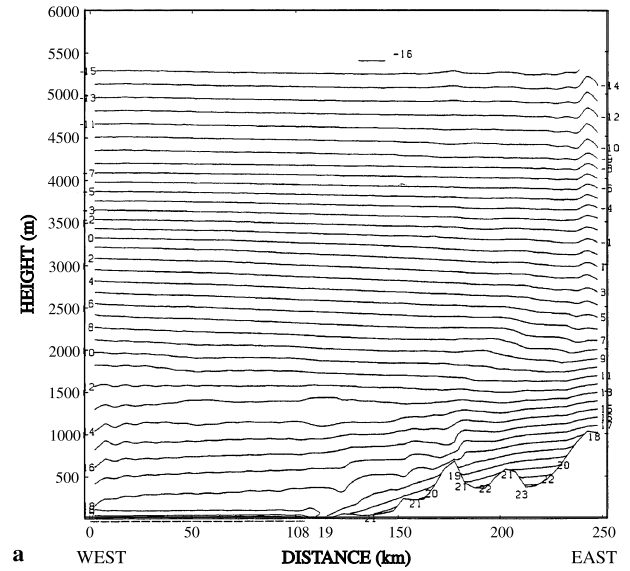


a WEST DISTANCE (km) EAST

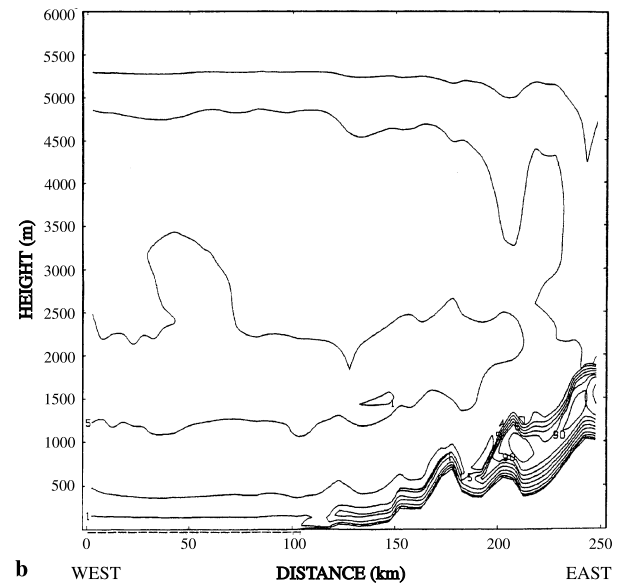


b WEST DISTANCE (km) EAST

Fig. 8a. Vertical wind profile (m s^{-1} , horizontal scale and cm s^{-1} , vertical scale) at 1800 LST, 20 May, 1998 on the line A–B in Fig. 7b. “Yel”, “Sea”, “In” and “Seo” denote the Yellow Sea, coastal sea, Incheon and Seoul cities, respectively. **(b)** as in **(a)**, except contours of vertical wind speed (cm s^{-1}). Negative values denote downward motion



a WEST DISTANCE (km) EAST



b WEST DISTANCE (km) EAST

Fig. 9. As in Fig. 8a, except for, **(a)** air temperature ($^{\circ}\text{C}$), and **(b)** vertical diffusion coefficient of turbulent heat ($\text{m}^2 \text{s}^{-1}$). The CBL is contained below the closely spaced lines

3.3 Atmospheric circulation and boundary layer (sunset)

From 1800 LST to 2100 LST, a high-pressure in the northern part of the Korean peninsula near Vladivostok, Russia produced a persistent synoptic westerly wind directed from the Yellow Sea into the Incheon coast. In the fine-mesh domain, an onshore wind associated with both a synoptic westerly wind and a sea breeze was directed toward the inland basin. This further combined with the valley wind directed from the inland basin toward the mountains and became an even stronger westerly wind across the Seoul metropolitan area and toward the top of the mountains (Figs. 7 and 8).

As indicated by the distribution of air temperature and vertical diffusion coefficient of heat, the depth of the CBL decreased slightly from the coast toward the inland basin and up to the mountains, compared to 1200 LST (Fig. 9). The shallower CBL could affect the depth and concentration of suspended particulates.

3.4 Dispersion of suspended particulate (sunset)

At 1700 LST, which is close to sunset, the CBL reduced in depth to 300 m due to the decrease in solar radiation, and became much shallower than at 1200 LST. As a result, the TSP concentration in the shallow CBL increased. An increase in the number of vehicles occurred on the roads after office hours (from 1700 LST), which resulted in an increase in the amount of

gases and particulates emitted. Consequently, the TSP concentration became very high (Figs. 10 and 11). After sunset (1800 LST), the number of vehicles gradually decreased and particulate emissions also decreased, resulting in a low TSP concentration.

As the amount of cooling at the surface shortly after sunset was not large, the nocturnal surface inversion layer was not much shallower than the convective boundary layer close to sunset. Under this condition, an easterly mountain wind directed toward the basin was not generated and westerly winds continued to transport the suspended particulates toward the mountains until 2000 LST. The tendency for a low concentration of particles in the model result closely matched the measured TSP concentration by MOE (1998). After sunset, the number of released particles in the model was reduced to two particles per two minutes from four particles per two minutes in the daytime, due to the reduced number of vehicles on the roads.

3.5 Nocturnal atmospheric circulation and boundary layer

Nocturnal radiative cooling of the surface can generally produce a wind directed from the top of mountains downslope toward the inland basin and a land breeze directed from the inland plain toward the sea, resulting in the generation of an offshore wind in the Seoul area. At 0000 LST, 21 May, a synoptic-scale westerly wind directed from the open sea toward the coastal

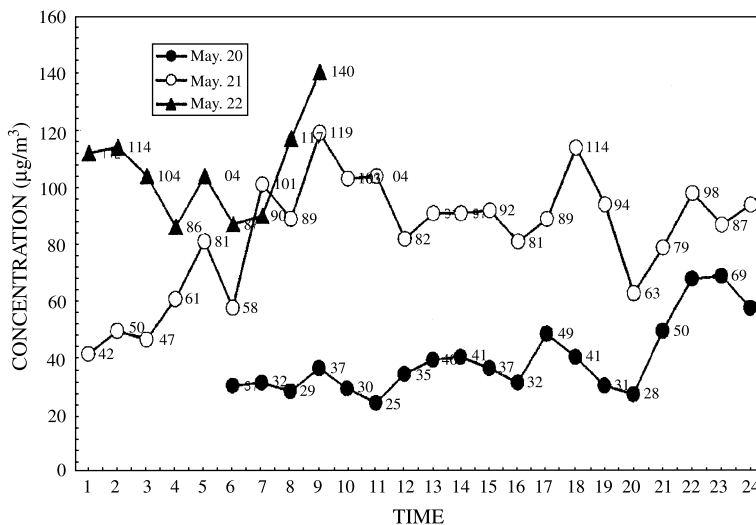
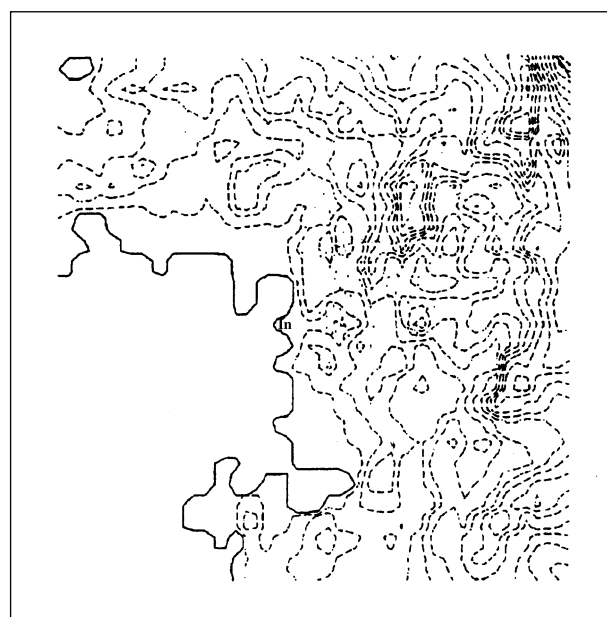
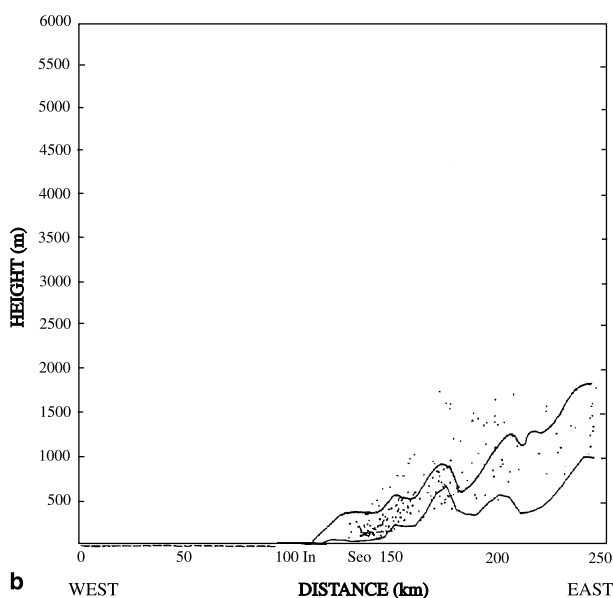


Fig. 10. Hourly concentration of total suspended particulate ($\mu\text{g m}^{-3}$) at Kangwamoon monitoring site in the Seoul metropolitan area from 20 May to 22 May, 1998



a

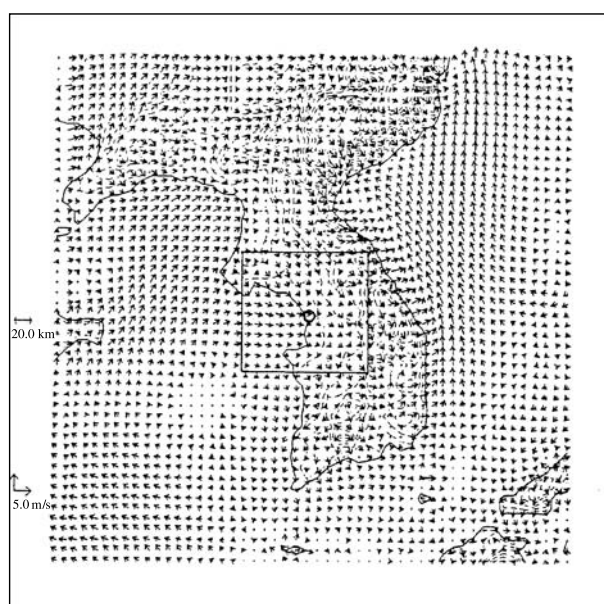


b

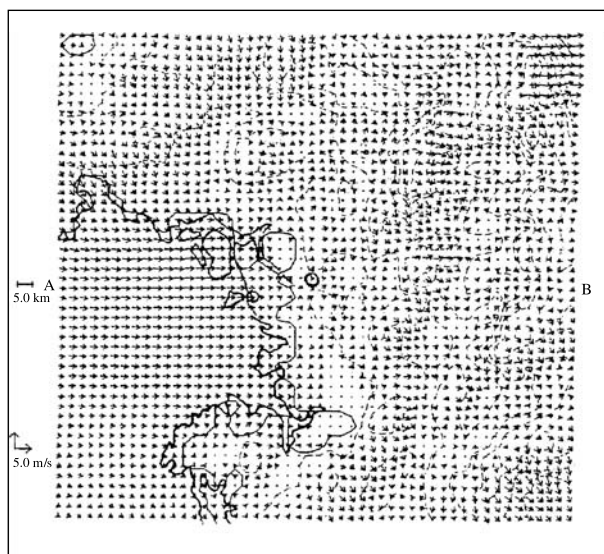
Fig. 11a. As in Fig. 6a, except at 1800 LST, on 20 May, 1998, twelve hours after releasing particulates. **(b)** as in **(a)**, except vertical cross-section through Incheon city and Seoul city. Upper and lower lines indicate the top of the CBL and topography, respectively

inland plain, that was induced by the high-pressure system, was interrupted offshore owing to the difference in nocturnal cooling rates of the surfaces. This resulted in a moderate wind speed near the coast (Fig. 12).

At the same time, a relatively weak westerly wind or calm conditions existed in the Seoul metropolitan area (Fig. 13). The vertical pro-



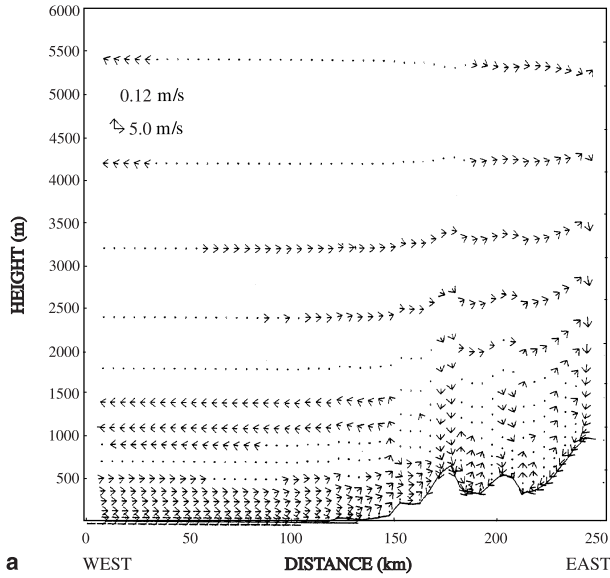
a



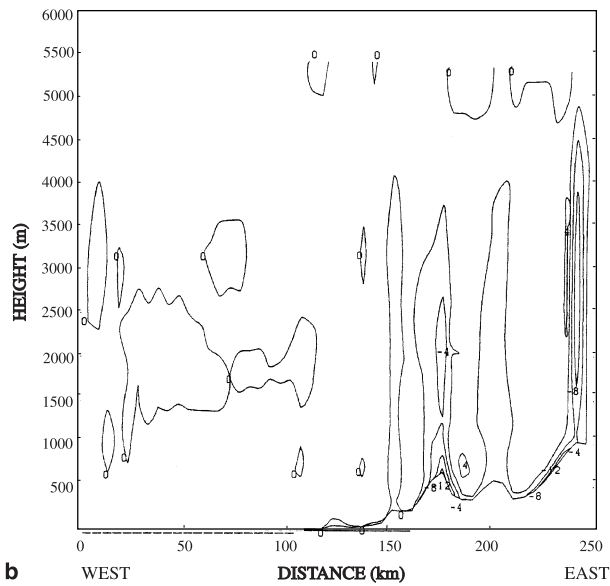
b

Fig. 12a. Wind vectors (m s^{-1}) 10 m above ground level at 0000 LST, May 21, 1998 in the coarse-mesh domain near the Korean peninsula and **(b)** as in **(a)** except in the fine-mesh domain focused around near Seoul city. Dashed lines denote topography. The two open circles denote Incheon city in **(a)** and Seoul city in **(b)**

files of vertical diffusion coefficient of turbulent heat ($\text{m}^2 \text{s}^{-1}$) indicate that nocturnal surface cooling produced a shallow nocturnal surface inversion layer (NSIL) approximately 200 m in thickness over the inland, but a relatively larger thickness of 300 m in the marine atmospheric inversion layer (MAIL). Also, a warm pool is evident over the Yellow Sea (Fig. 14). The air



a



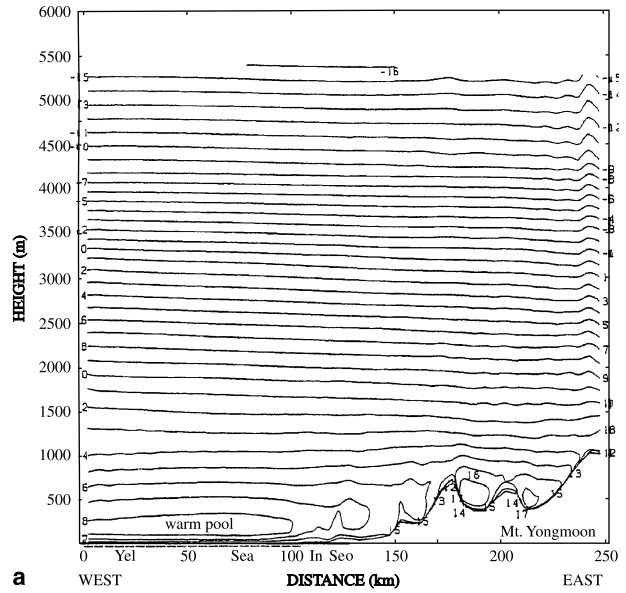
b

Fig. 13a. Vertical wind profile (m s^{-1} , horizontal scale and cm s^{-1} , vertical scale) on the line A–B in Fig. 12b at 0000 LST, 21 May, 1998. **(b)** as in (a), except contours of vertical wind speed (cm s^{-1}). Negative values imply downward motion

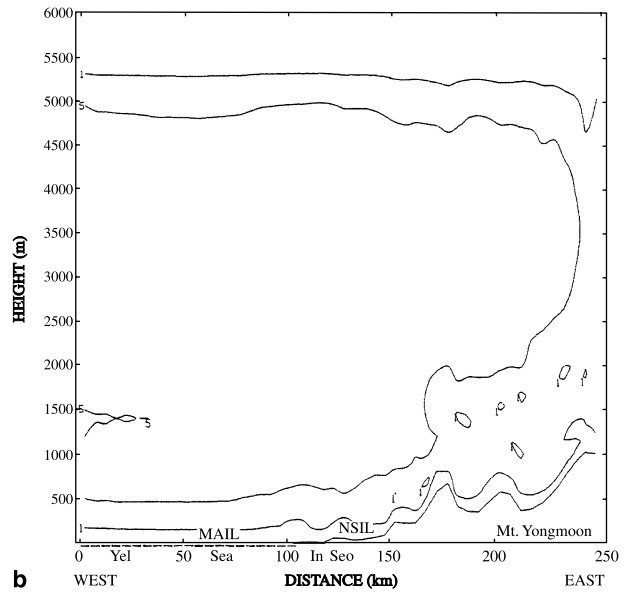
temperature near the surface in the downtown area at 0000 LST was 6°C lower than that at 1800 LST.

3.6 Nocturnal dispersion of suspended particulates

Since a downslope mountain wind after sunset penetrated the Seoul metropolitan area, the daytime suspended particulate matter also descended



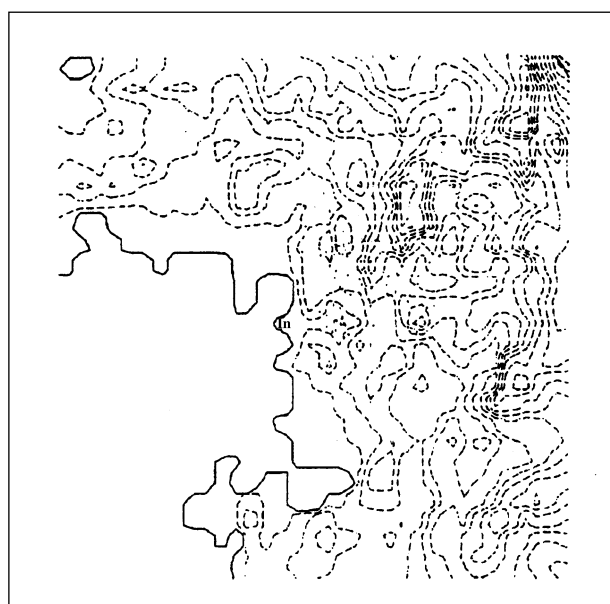
a



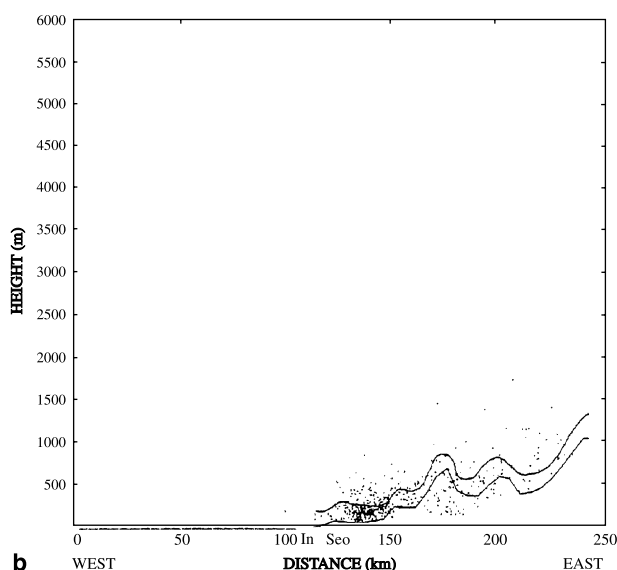
b

Fig. 14. As in Fig. 13, except **(a)** for air temperature ($^\circ\text{C}$) and **(b)** vertical diffusion coefficient of turbulent heat ($\text{m}^2 \text{s}^{-1}$). NSIL and MAIL denote nocturnal surface inversion layer and marine atmospheric inversion layer, respectively

both from the top of the shallow nocturnal surface inversion layer and from the western slope of the mountains toward the inland basin of Seoul city, causing a recycling of pollutants, which then merged with the particulate matter in the central part of the city (Fig. 15). The recycled particulates merged in the shallow NSIL and spread out at the surface level. As the nocturnal cooling at the surface increases, the depth of the nocturnal inversion layer decreases.



a



b

Fig. 15a. Plan view showing transport of particulates near Seoul city at 0000 LST, on 21 May, 1998, 18 hours after releasing particulates. “In” denotes Incheon city and the diamond shaped topographical contour to the right indicates Seoul city. **(b)** as in **(a)**, except vertical cross-section through Incheon city and Seoul city. Upper and lower lines indicate the top of the NSIL and topography, respectively

Thus the TSP concentration in the city continued to increase into the night. The maximum of recycled particulates in the city area and the nocturnal particulates continuously emitted at the surface of the city in the shallow NSIL, could enhance an already very high concentration of suspended particulates at about 0000 LST, with

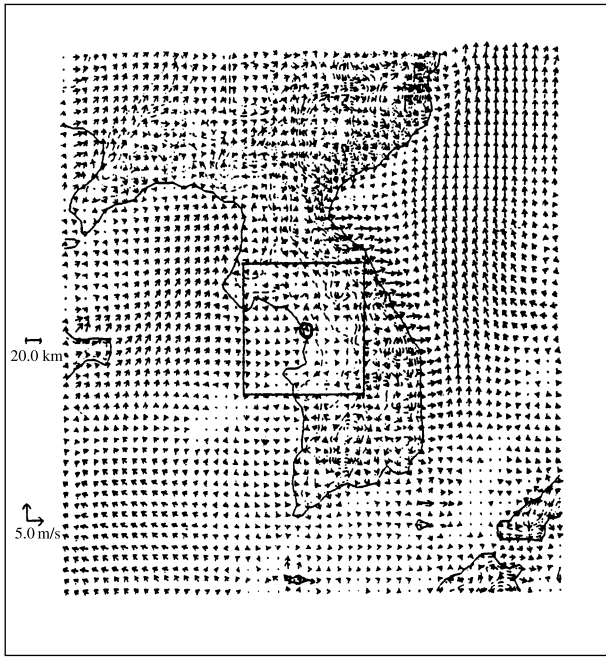
a maximum concentration occurring especially at 2300 LST (Figs. 10 and 15). The density of particulates calculated by the model showed a correct tendency to increase.

Close to midnight, these particulates moved toward the coast through the narrow channel of the western outlet of the Seoul city basin. As the particulates further dispersed across the coast by the land breeze, the TSP concentration in Seoul city became low, but high at the coast near Incheon city. Maximum nocturnal cooling at the surface occurred just before sunrise, resulting in the shallowest surface inversion layer at that time. Weak westerly winds prevented the advance of particulates transported from Seoul toward the sea, and the merging of particulates near the coast inside the inversion layer resulted in a high TSP concentration of $81 \mu\text{g m}^{-3}$ at 0500 LST.

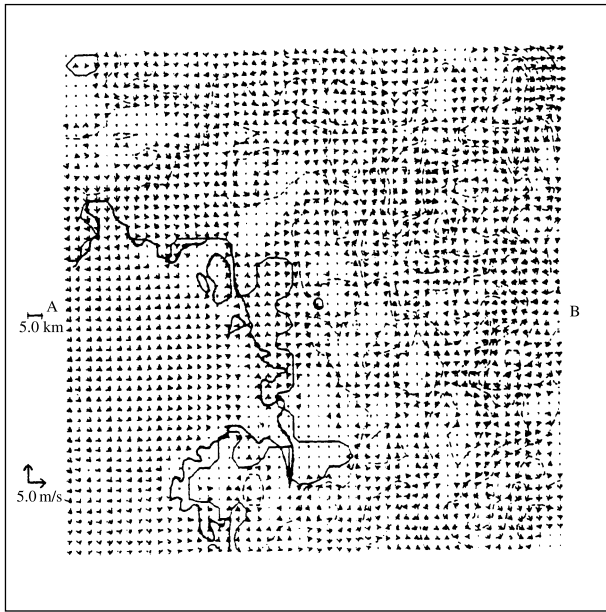
3.7 Atmospheric circulation and boundary layer (following morning)

At 0600 LST, the synoptic-scale wind was still westerly near the coast, and diffluence is evident in the southeast part of the Yellow Sea near the southwest coast of Korea (Figs. 16 and 17). Early in the morning, radiative cooling at the surface could produce a land-mountain breeze (katabatic) directed from the top of the mountains toward the sea. A westerly wind of only moderate speed occurred near the coast at 0600 LST owing to the suppression of the synoptic-scale westerly wind by the offshore wind, combined with the easterly katabatic wind. In the Seoul metropolitan area conditions were calm.

The westerly wind could transport particulates at the coast from the previous night toward the inland basin and Seoul metropolitan area, thereby establishing the recycling process as a very important driving mechanism for the occurrence of high TSP concentration in the early morning, as illustrated in Fig. 10. Sensible heat flux divergence occurred from the surface into the lower troposphere inducing the formation of a NSIL to a depth of about 200 m over the inland basin. The air temperature near the surface in the centre of Seoul was still low (Fig. 18a). The MAIL was also evident over the sea surface indicated by the warm pool of air (Fig. 18b). However, after 0600 LST, the synoptic-scale westerly wind



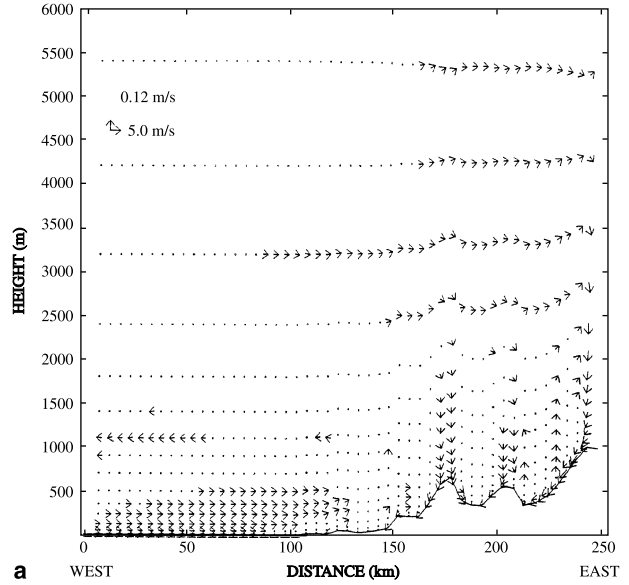
a



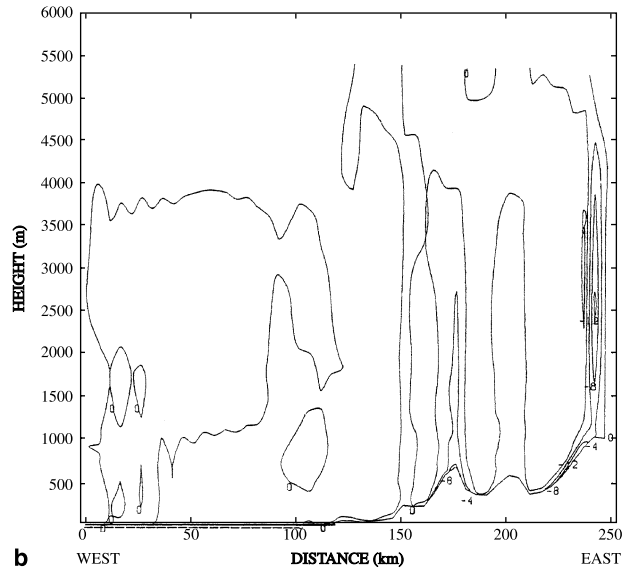
b

Fig. 16a. Wind vectors (m s^{-1}) 10 m above ground level in the coarse-mesh domain (20 km) near the Korean peninsula at 0600 LST, 21 May, 1998. The inset, small open circle and lines (dashed) denote the fine-mesh domain, Seoul city and topography, respectively. **(b)** as in **(a)** except in the fine-mesh domain (5 km). The small open circle denotes Seoul city. Dashed lines denote topography

combined again with the westerly sea-breeze and valley wind, and was directed from the coast toward the Seoul basin.



a

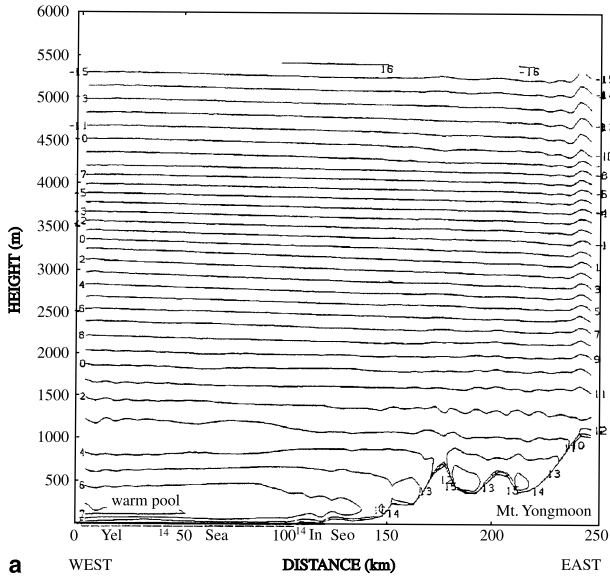


b

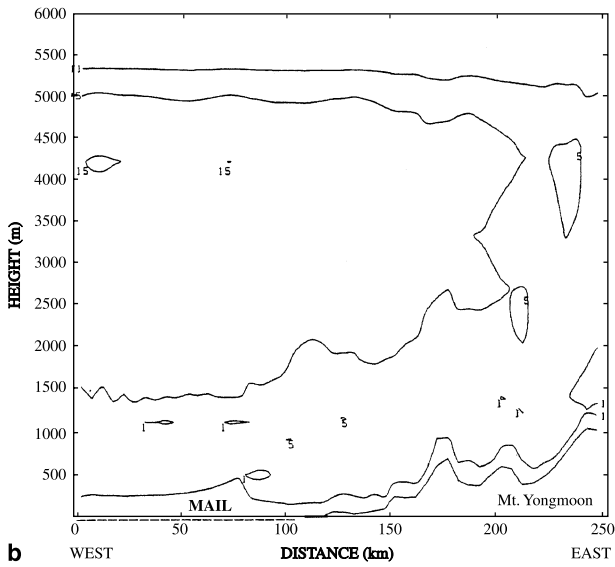
Fig. 17a. Vertical wind profile (m s^{-1} , horizontal scale and cm s^{-1} , vertical scale) on the line A-B in Fig. 16b at 0600 LST, 21 May, 1998. **(b)** as in **(a)** except contours of vertical wind speed (cm s^{-1}) with negative values denoting downward motion

3.8 Dispersion of suspended particulates (following morning)

In the MAIL, particulates tend to rise slightly because the depth of the MAIL is twice as large as the NSIL over the land near the coast. Thus, particulate concentration over the sea surface near the coast was lower relative to the concentration over the land near the coast. In the early morning the particulates transported by the



a

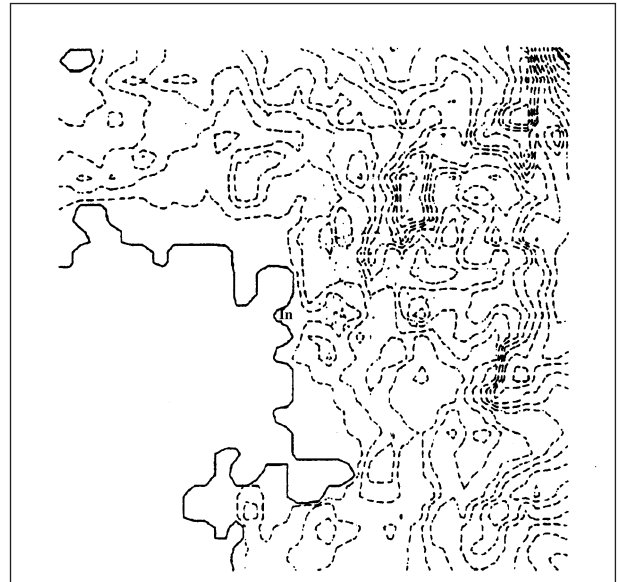


b

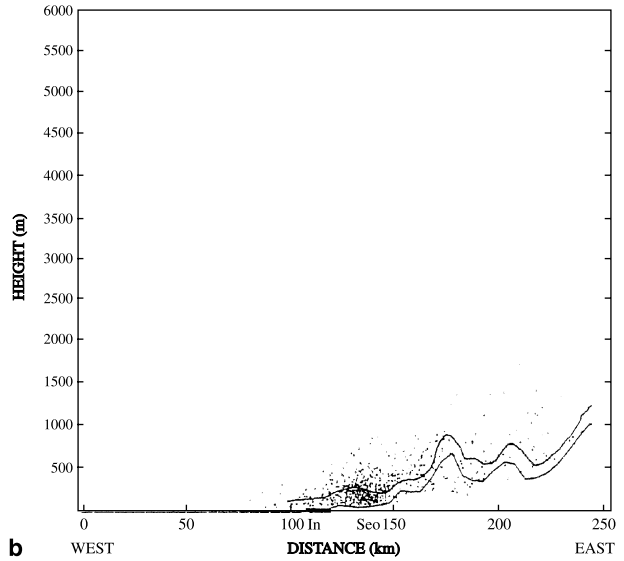
Fig. 18a. As in Fig. 17a, except for air temperature ($^{\circ}\text{C}$). (b) as in (a) except for vertical diffusion coefficient of turbulent heat ($\text{m}^2 \text{s}^{-1}$). “Yel”, “Sea”, “In” and “Seo” denote the Yellow Sea, coastal sea, Incheon city and Seoul city, respectively. MAIL denotes marine atmospheric inversion layer

easterly offshore wind reached the Yellow Sea in the west.

Just offshore, westerly winds above the top of the NSIL met easterly winds near the surface inside the inversion layer, resulting in a weak westerly surface wind. This weak westerly wind prohibited the advance of particulates transported from the city area toward the coast, resulting in a merging of particulates near the surface at the coast within the NSIL and hence, high concen-



a



b

Fig. 19a. Plan view showing recycled particulates having been transported over the coast from the previous night toward Seoul city (diamond topographical contour shape to the east of “In”) at 0600 LST, 21 May, 1998 by an onshore wind, 18 hours after releasing particulates in the model. (b) as in (a), except vertical cross-section through Incheon city and Seoul city indicating merging and vertical movement of both recycled and emitted particulates toward the top of the NSIL over Seoul city. Upper and lower lines indicate the top of NSIL and topography, respectively. “In” and “Seo” denote Incheon and Seoul cities, respectively

trations of TSP (greater than $80 \mu\text{g m}^{-3}$) until 0600 LST (Fig. 19).

At 0900 LST the following day, the particulates that were transported from inland toward

the coast overnight, were recycled into the central part of Seoul city under the intensified onshore westerly wind combined with the synoptic-scale westerly wind and sea-breeze. Moreover, both the recycled particulates transported from the coast into the Seoul basin and the particulates continuously emitted from sources close to the surface in the city merged within the TIBL at the coast where Incheon is located and inside the shallow convective boundary layer overlying Seoul city, thereby enhancing an already high TSP concentration.

Compared to the measured data by MOE (1998), recycled amounts of suspended particulate matter might reach approximately 50% of the total amount of TSP concentration (Fig. 10). Owing to the recycled particulates, the TSP concentration at 0900 LST, 21 May was two to three times higher than at 0900 LST, 20 May. After 0900 LST, those particulates rose again toward the top of convective boundary layer by thermal convection and then the westerly onshore wind caused them to disperse in the direction of the mountains, resulting in the low TSP concentration. However, this low concentration was still higher than on the previous day. Under persistent synoptic-scale westerly winds produced by a high-pressure system in the Yellow Sea, this pattern of increasing TSP concentration continued on 22 May.

4. Conclusions

Using three-dimensional meteorological and Lagrangian particle dispersion models, it was verified over a 48 hour period that the diurnal variation of TSP concentration in the Seoul metropolitan area was greatly affected by the atmospheric circulation and the depth of the atmospheric boundary layer. Since particulate matter initially emitted from the surface in the metropolitan area rose toward the top of the CBL and dispersed near the top of mountains, the ground level concentration of TSP over the metropolitan area was generally very low but relatively high in the mountains. The concentration increased at around sunset in the decreased CBL depth.

The particulates were transported toward the top of the mountains by an enhanced westerly wind and returned to the central part of the city under the influence of a katabatic easterly wind,

where they concentrated within a shallow NSIL. Thus, the TSP concentration in the city area continued to increase during nocturnal hours. The merged particulates in the city area and the continuously emitted ones at the surface in the shallow NSIL enabled very high concentrations of suspended particulate matter to accumulate before midnight. From about midnight, those particulates moved toward the coast through the narrow topographical channel or outlet west of the Seoul metropolitan area. As those particulates further dispersed over the adjacent sea under the influence of the land breeze, the total suspended particulate concentration remained low in Seoul city, but high at the coast. Nocturnal cooling at the surface reached a maximum just before sunrise. As a weak westerly wind over the sea adjacent to the coast prevented the advance of the particulates toward the sea, the particulates accumulated over the land between Seoul and the coast and the shallow surface inversion layer enhanced high TSP concentrations already there. After sunrise, the onshore westerly wind again transported the particulates into the Seoul metropolitan area, and the particulates emitted during the morning near the surface over the city, from vehicles in particular, contributed greatly to an already high TSP concentration in the hours after sunrise.

Acknowledgements

This work is supported by the Environmental Science Center, Peking University, China and Department of Atmospheric Environmental Sciences, Kangnung National University, Korea during the fiscal year 2001–2002.

References

- Baird C (1995) Environmental chemistry. New York; Freeman 484 pp
- Businger JA (1973) Turbulence transfer in the atmospheric surface layer. Proc. Workshop on Micrometeorology (D. A. Haugen, ed). Bull Amer Meteor Soc 54: 67–100
- Choi H (2001) Numerical prediction on fog formation affected by the Yellow Sea and mountain. J Korean Meteor Soc 37: 261–282
- Dearhoff JW (1978) Efficient prediction of ground surface temperature and moisture with inclusion of a layer of vegetation. J Geophys Res 38: 659–661
- Katayama A (1972) A simplified scheme for computing radiative transfer in the troposphere. Technical Report 6, Dept. of Meteor., U.C.L.A., 77 pp

- Kimura F (1983) A numerical simulation of local winds and photochemical air pollution (1): two-dimensional land and sea breeze. *J Meteor Soc Japan* 61: 862–878
- Kimura F, Arakawa S (1983) A numerical experiment of the nocturnal low-level jet over the Kanto plain. *J Meteor Soc Japan* 61: 848–861
- Kimura F, Takahashi S (1991) The effects of land-use and anthropogenic heating on the surface temperature in the Tokyo metropolitan area: numerical experiment. *Atmos Environ* 25: 155–164
- Klemp JB, Durran DR (1983) An upper condition permitting internal gravity wave radiation in numerical meso-scale models. *Mon Wea Rev* 111: 430–440
- Kuwagata T, Sumioka M (1991) The daytime PBL heating process over complex terrain in central Japan under fair and calm weather conditions. Part 3: Daytime thermal low and nocturnal thermal high. *J Meteor Soc Japan* 69: 91–104
- Lyons WA, Olsson LE (1973) Detailed mesometeorological studies of air pollution dispersion in the Chicago lake breeze. *Mon Wea Rev* 101: 387–392
- MOE (1998) Hourly measured data of atmospheric pollutants. Ministry of Environment, Korea, 150 pp
- Moller D (2001) Photooxidation capacity. Proc. Workshop on Local and Regional Contribution to Air Pollution and Local Radiative Balance in Asian Developing Countries. Guangzhou, China, p 16
- Monin AS (1970) The atmospheric boundary layer. *Ann Rev Fluid Mech* 2: 225–250
- NFRADA (1998) Analyzed NOAA satellite picture on the sea surface temperature. National Fisheries Research and Development Agency
- Orlanski I (1976) A simple boundary condition for unbounded hyperbolic flows. *J Comp Phys* 21: 251–269
- Park SU, Moon JY (2001) Lagrangian particle dispersion modeling in the complex coastal terrain of Korea. *J Korean Meteor Soc* 37: 225–238
- PU (1995) The effects of particles and gases on acid depositions and parameterization. Technical Report of State Key Project, 85-912-01-04-05, 250 pp
- Ross DG, Lewis AM, Koutsenko GD (1999) Comalco (Bell Bay) local airborne contaminant transport study: airshed modeling system, development and evaluation. Proc. 5th Joint Seminar on Regional Deposition Process in the Atmosphere, Seoul, pp 43–52
- Seinfeld JH, Pandis SN (1998) Atmospheric chemistry and physics: From air pollution to climate change. New York: Wiley, 1326 pp
- Takahashi S (1998) Manual of LAS model revised by Dr. Sato, J., 50 pp
- Xuan J (1999) Vertical fluxes of dust in northern Asia. Proceedings of fifth joint seminar on regional deposition process in the atmosphere, Seoul, pp 43–52
- Yamada T (1983) Simulation of nocturnal drainage flows by a q2-1 turbulence closure model. *J Atmos Sci* 40: 91–106
- Yamada T, Mellor GL (1983) A numerical simulation of the BOMEX data using a turbulence closure model coupled with ensemble cloud relations. *Q J R Meteor Soc* 105: 95–944

Corresponding author's address: Hyo Choi, Department of Atmospheric Environmental Sciences, Kangnung National University, Kangnung 210-702, Korea (E-mail: choihyo@kangnung.ac.kr; du8392@hanmail.net)